Journal of Crystal Growth 310 (2008) 4908–4912

Contents lists available at ScienceDirect

Journal of Crystal Growth

journal homepage: www.elsevier.com/locate/jcrysgro

Effect of an Al_2O_3 transition layer on InGaN on ZnO substrates by organometallic vapor-phase epitaxy

Nola Li [a], Shen-Jie Wang [a], Chung-Lung Huang [b], Zhe Chuan Feng [b], Adriana Valencia [c], Jeff Nause [c], Christopher Summers [d], Ian Ferguson [a,*,1]

[a] School of Electrical and Computer Engineering, Georgia Institute of Technology, 778, Atlanta, GA 30332, USA
[b] Graduate Institute of Photonics and Optoelectronics and Department of Electrical Engineering, National Taiwan University, Taipei, Taiwan 106-17, ROC
[c] CERMET Inc., 1019 Collier Road, Atlanta, GA 30318, USA
[d] School of Materials Science and Engineering, Georgia Institute of Technology, Atlanta, GA 30332, USA

ARTICLE INFO

Available online 5 August 2008

Keywords:
A1. X-ray diffraction
A3. Organometallic vapor phase
B1. Nitrides
B1. ZnO substrate
B2: Semiconducting materials

ABSTRACT

InGaN was grown on bare ZnO as well as Al_2O_3 deposited ZnO substrates by organometallic vapor-phase epitaxy (OMVPE). The Al_2O_3 transition layer was grown by atomic layer deposition (ALD) in order to prevent Zn and O diffusion from the ZnO substrate and promote nitride growth. *In-situ* annealing of the transition layer was first performed right before InGaN growth in the chamber. High-resolution X-ray diffraction (HRXRD) measurements revealed that the thin Al_2O_3 layer after annealing was an effective transition layer for the InGaN films grown epitaxially on ZnO substrates. Optical transmission (OT) was performed to measure the bandgap energy using Sigmoidal fitting. Auger electron spectroscopy (AES) atomic depth profile shows a decrease in Zn in the InGaN layer. The diffusivity of Zn in the GaN layer grown on the bare ZnO substrate is about $5\times10^{-16}\,cm^2/s$. Moreover, (0 0 0 2) InGaN layers were successfully grown on 20 nm Al_2O_3/ZnO substrates after 10 min annealing in a high-temperature furnace.

1. Introduction

ZnO is an ideal substrate for epitaxial growth of GaN and InGaN. It has the same wurtzite structure with only a 1.8% *c*-plane lattice mismatch with GaN. InGaN, with a composition of 18% indium, has a perfect lattice-match with ZnO in the *a*-axis direction, which allows for the possible growth of InGaN layers without misfit dislocations [1–3]. In addition, ZnO substrates are conductive so can be utilized in vertical structures allowing for multiple electrodes to be formed on both surfaces to further current spreading [4,5]. Furthermore, ZnO can be wet-etched chemically and easily removed to allow for a thin nitride structure [6]. Molecular beam epitaxy (MBE) and pulse laser deposition (PLD) techniques have been employed to realize the low-temperature epitaxy of GaN-based materials on ZnO substrates [1,2,7]. However, organometallic vapor-phase epitaxy (OMVPE) is currently the dominant growth technology for GaN-based materials and devices, and there is a need to explore this technique for ZnO substrates. OMVPE growths of GaN are grown at high temperatures where ZnO substrates decompose causing diffusion of Zn and O into the epilayers. This issue has been demonstrated by secondary ion mass spectrometry (SIMS) depth profile of the GaN/ZnO interface [8,9]. The diffusion can cause poor epitaxial growth and degrade the film quality. It has been reported that the Zn doping in the GaN layer forms a deep level inducing red-shift emission of 0.5 eV [10]. Moreover, the same observation has also been reported for Zn diffusion into InGaN layers from the ZnO substrate [3].

A transition layer was grown between the ZnO substrate and the InGaN epilayer in order to prevent Zn and O diffusion, protect the ZnO surface from H_2 back etching due to pyrolysis of NH_3, and promote nitride growth. Al_2O_3 was chosen as the transition material due to its transparency, excellent thermal stability (in contrast to ZnO), and because it is a readily available material that can be deposited by atomic layer deposition (ALD) [11]. ALD was chosen as the growth method due to its ability to obtain a smooth surface and more accurate thickness control on ZnO. This method allows for smooth layer deposition with low pinhole density and good uniformity over large area substrates. Furthermore, the thickness is accurately controlled just by the number of growth cycles rather than temperature, etc [12,13]. Post-annealing will be performed on as-deposited Al_2O_3 films in order to transfer to crystallize the layer for subsequent InGaN growth.

* Corresponding author. Tel.: +1 404 385 2885.
E-mail addresses: zcfeng@cc.ee.ntu.edu.tw (Z.C. Feng), ianf@ece.gatech.edu (I. Ferguson).
[1] Also with School of Materials Science and Engineering, Engineering, Georgia Institute of Technology (GaTech), Atlanta, GA 30332, USA.

0022-0248/$ - see front matter © 2008 Published by Elsevier B.V.
doi:10.1016/j.jcrysgro.2008.07.087

This paper will discuss growth of InGaN layers by OMVPE on bare ZnO substrates in order to optimize the layer before growth on annealed Al_2O_3/ZnO substrates. Results of InGaN on an *in-situ* annealed transition layer will show that the transition layer was able to allow for the InGaN growth as well as reducing Zn diffusion. This paper will also go into the beginnings of furnace annealing followed by OMVPE InGaN growth.

2. Experimental procedures

InGaN layers were grown on bare ZnO substrates and then transferred to annealed 20 nm Al_2O_3/ZnO substrates with various annealing time by OMVPE in a modified commercial rotating disk reactor with dual injector blocks. The GaN buffer layer was grown at 530 °C with a thickness of 30 nm using trimethylgallium (TMGa) and ammonia (NH_3) as the gallium and nitrogen sources, respectively. Following the buffer layer, growth of InGaN layers of about 100 nm thick at 700 °C with a growth rate of 0.18 μm/h by introducing trimethylindium (TMIn) and triethylgallium (TEGa) into the reactor. N_2 carrier gas was used during the whole growth process.

Al_2O_3 films of 5 and 20 nm were grown on the Zn face of ZnO (0 0 0 1) substrates at a temperature of 100 °C using a quartz tube with trimethylaluminum (TMAl) and H_2O as the precursors. ALD is a process where single precursors are pulsed into the reactor separated alternately by purging of N_2 or evacuation periods. The film growth took place in a cyclic manner at a base pressure of 500 mTorr. One growth cycle consisted of four consecutive steps: (1) exposure to the metal precursor TMAl, (2) N_2 purge, (3) exposure to H_2O, and (4) another N_2 purge. This method allows for a self-limited layer-by-layer growth mode.

Annealing of the 5 nm Al_2O_3 layer was first performed *in-situ* right before InGaN growth by OMVPE. These layers showed promise for InGaN growth with less Zn diffusion from the ZnO substrate. Further annealing studies were done in a furnace at higher temperatures of greater than 1200 °C at different times in a N_2 ambient in order to study the crystallization characteristics of the Al_2O_3 film. The structures of the post-annealed Al_2O_3 films as well as the subsequent InGaN film were characterized by high-resolution X-ray diffraction (HRXRD) using a Philips X'Pert MRD diffractometer. Rutherford backscattering (RBS) was employed to determine the film composition and thickness. The optical bandgap of InGaN was estimated from the optical transmission (OT) spectra. Atomic depth profile was measured by Auger electron spectroscopy (AES), respectively.

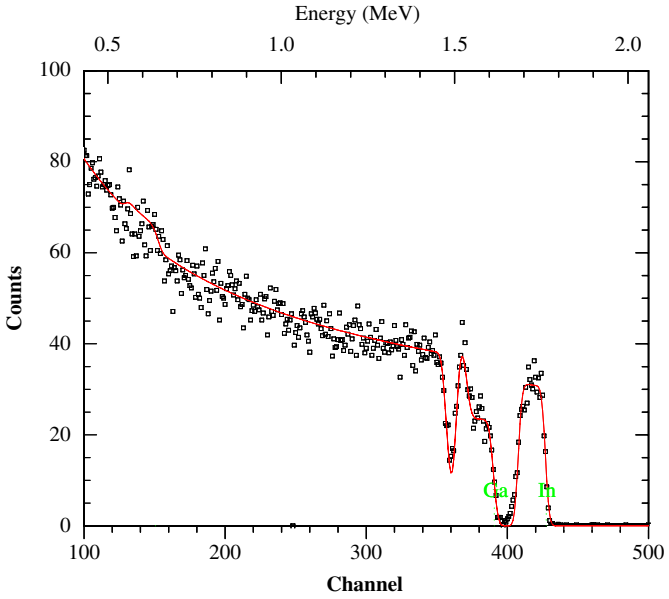

Fig. 1. Random (square) and simulated (solid line) RBS spectra of InGaN/GaN/ZnO sample.

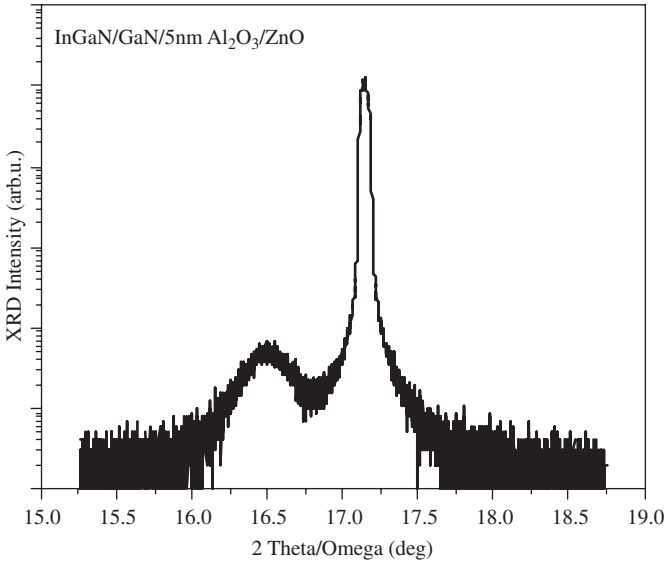

Fig. 2. HRXRD $2\theta/\omega$ scan of InGaN layers grown on *in-situ* annealed 5 nm Al_2O_3/ZnO substrate.

3. Results and discussion

3.1. Optimization of InGaN layer grown on bare ZnO substrates

Initial InGaN layers were grown on bare ZnO substrates with a GaN buffer layer in order to find an optimal growth condition to transfer to annealed Al_2O_3/ZnO substrates. Successful growths of InGaN layers on bare ZnO with high indium composition were confirmed by HRXRD in a previous study [3]. Random RBS spectra have been performed on the InGaN/GaN/ZnO structures in order to confirm the indium composition as well as the thickness of each individual layer, Fig. 1. The energy for backscattering of both Ga and In at the surface has been labeled. A simulation of the random spectrum reveals that the good quality InGaN layer has an indium composition as high as 35% and a thickness of about 80 nm. Moreover, the thickness of the GaN buffer layer was estimated from a random spectrum as 35 nm. These values of composition and thickness are close to the numbers that were measured by HRXRD and *in-situ* reflectance curve.

3.2. Epitaxial growth of InGaN layers on in-situ annealed 5 nm Al_2O_3/ZnO substrates

In-situ annealing of a 5 nm Al_2O_3/ZnO substrate at 900 °C for 20 min in N_2 ambient was attempted in the OMVPE chamber right before growth of the InGaN layer. The $2\theta/\omega$ HRXRD scan shows two well-separated peaks from the ZnO substrate and InGaN layer, as shown in Fig. 2. The concentration of indium from the InGaN layer was calculated by the shift of the (0 0 0 2) InGaN peak position relative to the (0 0 0 2) ZnO peak position via Vagard's law. A single phase of InGaN, grown on annealed Al_2O_3/ZnO substrate, was obtained with an indium concentration of 32%, as identified by HRXRD. It is indicated that the InGaN layer can be epitaxially grown on Al_2O_3 deposited ZnO substrate after

crystallization. OT measurements were also performed on InGaN layers grown on bare ZnO and annealed Al_2O_3/ZnO substrates (Fig. 3). There are two obvious steps in each curve, corresponding to the absorption edge of ZnO and InGaN, respectively. Both spectra exhibit a very sharp and transmission wavelength edge at 387 nm, which was attributed to the underlying ZnO substrates. Moreover, the InGaN optical absorption edge can be determined by the sigmoidal fitting seen in [14,15]

$$T(E) = \frac{T_0}{1 + \exp(E_g - E/\Delta E)} \quad (1)$$

where T is the transmission, E_g is identified as the bandgap of the alloy, and ΔE is the broadening parameter, which is equivalent to the Urbach tailing energy. Both of the bandgaps for InGaN grown on bare ZnO and on annealed Al_2O_3/ZnO substrates have been calculated to be about 2.43 and 2.51 eV, respectively. It is indicated that the bandgap energy of InGaN was not altered significantly when grown on annealed Al_2O_3/ZnO substrates. Taking the bandgap of InGaN on 5 nm Al_2O_3/ZnO and putting it into the following equation: $E_g(\text{strained}) = 3.42 - 0.65x - 3.4159x(1-x)$ where $E_g = 2.43$ eV gives 34% indium concentration, which is close to the HRXRD measurement [16].

3.3. AES atomic depth profiles of the InGaN layers

The atomic depth profiles of InGaN layers grown on bare ZnO and 5 nm annealed Al_2O_3/ZnO substrates are shown in Fig. 4(a and b). The diffusion of Zn can be clearly observed from the ZnO substrate into the InGaN layer for both cases, as seen in Fig. 4(a). The concentration of Zn in the InGaN layer grown on bare ZnO substrate is around 0.7 at%. Moreover, the concentration of Zn is reduced to 0.3 at% when grown on annealed Al_2O_3/ZnO substrate, Fig. 4(b). It is noticed that the 5 nm Al_2O_3 can retard the Zn diffusion but the amount of Zn-content still needs to be further reduced. The Zn diffusivity was also evaluated in the case of bare ZnO substrates. The schematic diagram of the InGaN/GaN/ZnO structure can be seen in Fig. 5. The Zn atomic flux from the ZnO substrate into the InGaN layer can be calculated by [17]

$$J_{Zn} = \frac{TA\rho f_{zn} N_0}{M_{Zn} tA} \quad (2)$$

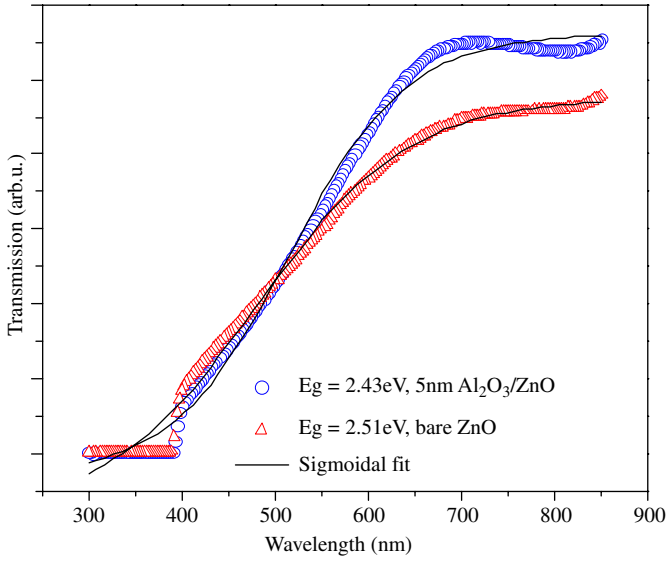

Fig. 3. OT spectra of InGaN layers grown on bare ZnO and annealed 5 nm Al_2O_3/ZnO substrate.

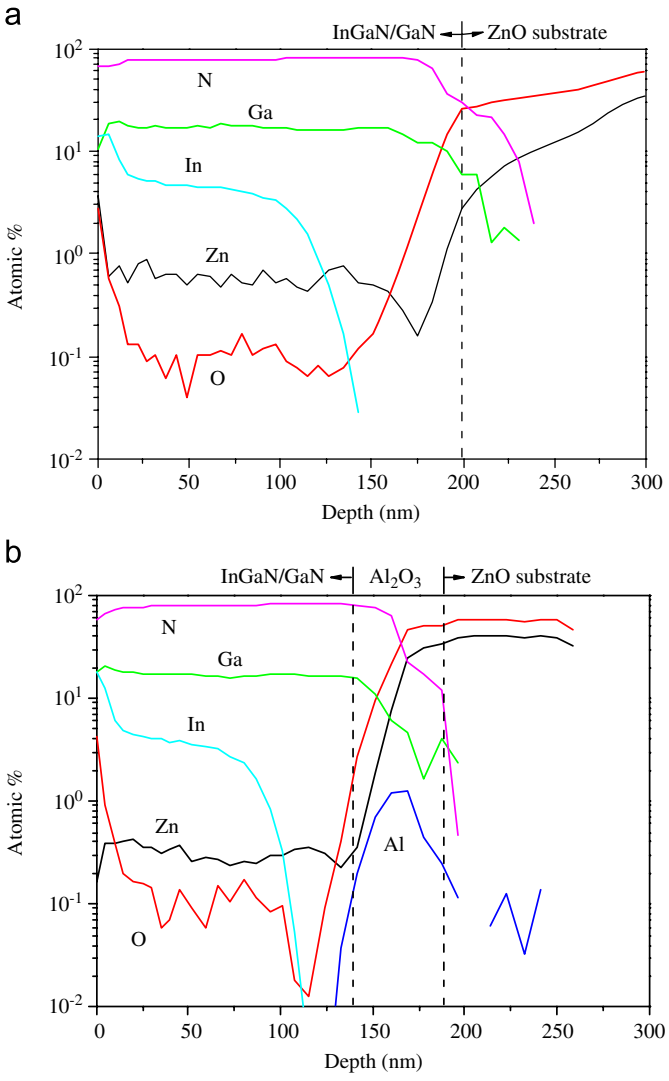

Fig. 4. AES atomic depth profile of InGaN layers grown on (a) bare ZnO and (b) annealed 5 nm Al_2O_3/ZnO substrate.

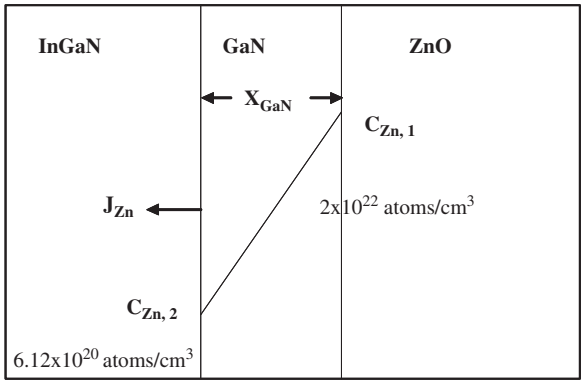

Fig. 5. Schematic drawing of the interfaces for Zn atomic flux calculation from the bare ZnO substrate into the InGaN layer.

where T is the InGaN thickness; A the epilayer area; ρ the density of InGaN with 32%In, 6.3 (g/cm^3); f_{Zn} the Zn weight fraction in InGaN, 0.01; N_0 the Avogadro's number; t represents the growth time, 30 min; and M_{Zn} the atomic weight of Zn. Substitution of all the values above in Eq. (1) yields $J_{Zn} = 2.75 \times 10^{12}$ (atom/cm^2 s). The Zn atomic flux in the GaN buffer layer, J_{Zn}, also can be

expressed by Fick's second law assuming the Zn concentration gradient is linear. Therefore, the diffusivity of Zn in the GaN can be obtained by [18]

$$J_{Zn} = D_{Zn}\frac{C_{Zn,2} - C_{Zn,1}}{\chi_{GaN}} \quad (3)$$

where D_{Zn} is the Zn diffusivity in the GaN, χ_{GaN} the thickness of the GaN layer, $C_{Zn,1}$ the theoretical Zn concentration in ZnO (2×10^{22} atoms/cm^3), and $C_{Zn,2}$ the Zn concentration in InGaN (6.12×10^{20} atoms/cm^3), which can be obtained from the AES atomic depth profile. Therefore, D_{Zn} is calculated to be about 2.37×10^{-16} cm^2/s. This diffusivity of Zn in GaN at 700 °C is in the same order as the Zn diffusivity in GaN at 930 °C (1×10^{-16}) [19]. The concentration of O in the InGaN layer was at a consistent value of 0.1% with and without the Al_2O_3 film deposited. The thicknesses marked in Fig. 4 are only observations. Fig. 4(a) might have different thicknesses due to etching of the ZnO substrate during growth, which induces the non-uniformed interface of each individual layer. The Al_2O_3 spreading in Fig. 4(b) could be caused by post-annealing and diffusion during epilayer growth. Therefore, its thickness during atomic depth profile measuring could seem larger. Further study still needs to be performed.

3.4. Epitaxial growth of InGaN layers on furnace annealed Al_2O_3/ZnO substrates

Furnace annealing was used moving forward in order to anneal at higher temperatures as high as 1100 °C. The furnace also allows for a cleaner environment for annealing compared to the growth chamber which has deposition from previous growths that could contaminate the sample. A thicker layer of Al_2O_3 at 20 nm was grown in order to prevent Zn diffusion into the InGaN epilayer. Al_2O_3 films of 20 nm were deposited on ZnO substrates and then annealed at 10, 20, and 40 min at 1100 °C. HRXRD result shows the (0 0 2) and (0 0 4) peaks of the ZnO substrate as can be seen in Fig. 6. Additional peaks of interest are located at 38°, 44.5°, 52.5°, and 82°, which were assigned to the planes (1 1 0), (1 1 3), (0 2 4), and (3 0 6) of the α-Al_2O_3 phase from the JCPDS database for 10 min annealing. However, the (1 1 3) plane disappeared and the peak intensities of (0 2 4) and (3 0 6) planes became weaker after 20 min of annealing. Furthermore, the (0 2 4) plane vanished after 40 min of annealing. Therefore, the optimal annealing time at 1100 °C for crystallization may be at 10 min where the maximum number and highest intensity for the peaks can be obtained.

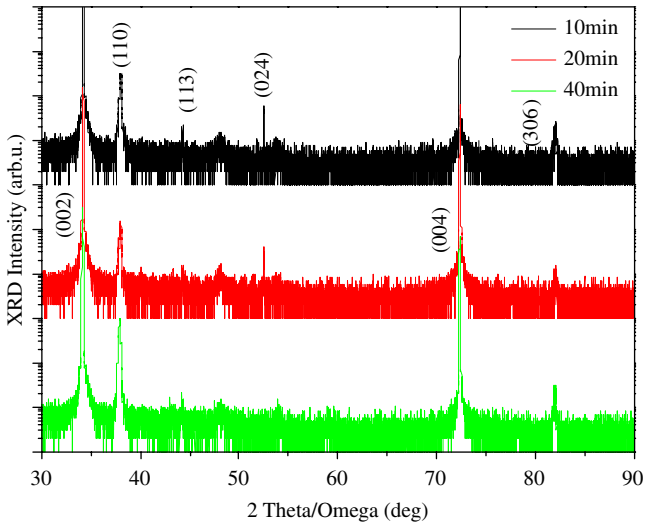

Fig. 6. HRXRD results of 20 nm Al_2O_3 films deposited on ZnO substrates by ALD annealed at 1100 °C for 10, 20, and 40 min.

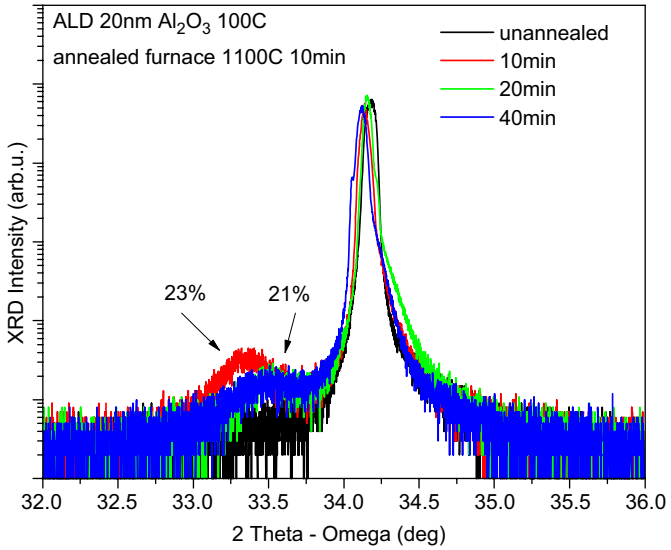

Fig. 7. HRXRD $2\theta/\omega$ scan of InGaN layers grown on 20 nm Al_2O_3/ZnO substrates at 1100 °C with various annealing times for 0, 10, 20, and 40 min.

InGaN (0 0 0 2) diffraction peaks were obtained on the 20 nm Al_2O_3/ZnO substrates at 1100 °C for 0, 10, 20, and 40 min, as seen in Fig. 7. It was also seen that the intensity of the InGaN peaks decreased with increasing annealing time. Moreover, no InGaN (0 0 0 2) peak was seen on the un-annealed sample. Shifts seen in the InGaN peaks denote different indium incorporation. This could be due to the different surfaces being grown on, which will change the nucleation density as well as the growth mode of the subsequent GaN and InGaN epilayer. Therefore, the indium composition can be changed due to the surface differences. The detail mechanism still needs to be studied.

4. Conclusions

Random RBS spectra and simulation data revealed that the InGaN layer on bare ZnO has an indium composition as high as 35 at% 80 nm. InGaN grown on *in-situ* annealed Al_2O_3/ZnO substrate showed a promising InGaN layer of 32% indium as identified by HRXRD. OT measurements showed that InGaN grown on both bare and 5 nm Al_2O_3/ZnO have a bandgap of 2.43 and 2.51 eV. Furthermore, AES atomic depth profiling showed the Zn concentration in the InGaN layer dropped from 0.7 to 0.3 at% with the use of the 5 nm Al_2O_3 transition layer. It is indicated that the transition layer was able to reduce Zn diffusion from the ZnO substrate into InGaN layer. The diffusivity of Zn in the GaN layer grown on the bare ZnO substrate is about 5×10^{-16} cm^2/s at 700 °C. InGaN layers were successfully grown on 20 nm Al_2O_3/ZnO substrates after 10 min annealing at 1100 °C in a high-temperature furnace.

Acknowledgments

This work was supported by the Department of Energy (DE-FC26-06NT42856). The work at National Taiwan University was supported partially by funds of NSC95-2221-E-002-118- and NSC96-2221-E002-166.

References

[1] A. Kobayashi, J. Ohta, H. Fujioka, J. Appl. Phys. 99 (2006) 123513.
[2] G. Namkoong, S. Burnham, K. Lee, E. Trybus, W.A. Doolittle, M. Losurdo, P. Capezzuto, G. Bruno, B. Nemeth, J. Nause, Appl. Phys. Lett. 87 (2005) 184104.
[3] S.J. Wang, N. Li, E.H. Park, S.C. Lien, Z.C. Feng, A. Valencia, J. Nause, I. Ferguson, J. Appl. Phys. 102 (2007) 106105.
[4] G.H.B. Thompson, Physics of Semiconductor Laser Devices, Wiley, New York, 1980, p. 307.
[5] A. Zukauskas, M.S. Shur, R. Gaska, Introduction to Solid-State Lighting, Wiley, New York, 2002 (p. 75).
[6] C.L. Chang, Y.C. Chuang, C.Y. Liu, Electrochem. Solid-State Lett. 10 (2007) 344.
[7] X. Gu, M.A. Reshchikov, A. Teke, D. Johnstone, H. Morkoc, B. Nemeth, J. Nause, Appl. Phys. Lett. 84 (2004) 2268.
[8] G. Popovici, W. Kim, A. Botchkarev, H. Tang, H. Morkoc, J. Solomon, Appl. Phys. Lett. 71 (1997) 3385.
[9] T. Suzuki, C. Harada, H. Goto, T. Minegishi, A. Setiawna, H.J. Ko, M.W. Cho, T. Yao, Curr. Appl. Phys. 4 (2004) 643.
[10] S. Nakamura, J. Crystal Growth 145 (1994) 911.
[11] L. Zhang, H.C. Jiang, C. Liu, J.W. Dong, P. Chow, J. Phys. D: Appl. Phys. 40 (2007) 3707.
[12] S. Jakschik, U. Schroeder, T. Hecht, M. Gutsche, H. Seidl, J.W. Bartha, Thin Solid Films 425 (2003) 216.
[13] M. Ritala, M. Leskela, Handbook of Thin Film Materials: Deposition and Processing of Thin Films ALD, Academic Press, San Diego, 2002 (p. 103).
[14] F.B. Naranjo, M.A. Sanchez-Garcia, F. Calle, E. Calleja, B. Jenichen, K.H. Ploog, Appl. Phys. Lett. 80 (2002) 231.
[15] S. Pereira, M.R. Correia, T. Monteiro, E. Pereira, M.R. Soares, E. Alves, J. Crystal Growth 230 (2001) 448.
[16] C.A. Parker, J.C. Roberts, S.M. Bedair, M.J. Reed, S.X. Liu, N.A. El-Masry, L.H. Robins, Appl. Phys. Lett. 75 (1999) 2566.
[17] S.J. Wang, C.Y. Liu, J. Elect. Mater. 32 (2003) 1303.
[18] S.J. Wang, C.Y. Liu, J. Elect. Mater. 35 (2006) 1955.
[19] H. Haneda, T. Ohgaki, I. Sakaguchi, H. Ryoken, N. Ohashi, A. Yasumori, Appl. Surf. Sci. 252 (2006) 7265.